Zinc-finger-based transcriptional repression of rhodopsin in a model of dominant retinitis pigmentosa

Claudio Mussolino[1†], Daniela Sanges[1], Elena Marrocco[1], Ciro Bonetti[1], Umberto Di Vicino[1], Valeria Marigo[2], Alberto Auricchio[1,3], Germana Meroni[1‡], Enrico Maria Surace[1]*

Despite the recent success of gene-based complementation approaches for genetic recessive traits, the development of therapeutic strategies for gain-of-function mutations poses great challenges. General therapeutic principles to correct these genetic defects mostly rely on post-transcriptional gene regulation (RNA silencing). Engineered zinc-finger (ZF) protein-based repression of transcription may represent a novel approach for treating gain-of-function mutations, although proof-of-concept of this use is still lacking. Here, we generated a series of transcriptional repressors to silence human rhodopsin (*hRHO*), the gene most abundantly expressed in retinal photoreceptors. The strategy was designed to suppress both the mutated and the wild-type *hRHO* allele in a mutational-independent fashion, to overcome mutational heterogeneity of autosomal dominant *retinitis pigmentosa* due to *hRHO* mutations. Here we demonstrate that ZF proteins promote a robust transcriptional repression of *hRHO* in a transgenic mouse model of autosomal dominant *retinitis pigmentosa*. Furthermore, we show that specifically decreasing the mutated human RHO transcript in conjunction with unaltered expression of the endogenous murine *Rho* gene results in amelioration of disease progression, as demonstrated by significant improvements in retinal morphology and function. This zinc-finger-based mutation-independent approach paves the way towards a 'repression–replacement' strategy, which is expected to facilitate widespread applications in the development of novel therapeutics for a variety of disorders that are due to gain-of-function mutations.

INTRODUCTION

Proof-of-concept studies and the recent success of clinical trials are providing sound evidence for the use of gene-based complementation therapeutic strategies to treat genetic recessive traits (Aiuti et al, 2009; Bainbridge et al, 2008; Cartier et al, 2009; Hauswirth et al, 2008; Kaplitt et al, 2007; Maguire et al, 2009, 2008). Nevertheless, the design of effective therapeutic strategies for dominant genetic traits still poses difficulties. The common therapeutic approach to correct these genetic entities relies on the silencing of gene expression. The main target of genetic silencing strategies is the messenger RNA (mRNA) transcript, the function of which can be inhibited by antisense-

(1) Telethon Institute of Genetics and Medicine (TIGEM), Naples, Italy.
(2) Department of Biomedical Sciences, University of Modena and Reggio Emilia, Modena, Italy.
(3) Medical Genetics, Department of Pediatrics, "Federico II" University, Naples, Italy.

*Corresponding author: Tel: +39 0816 132 334; Fax: +39 0815 790 919; E-mail: surace@tigem.it
† Present address: Department of Experimental Hematology, Hannover Medical School (MHH), Hannover, Germany.
‡ Cluster in Biomedicine – CBM S.c.r.l. AREA Science Park, Basovizza, Trieste, Italy.

RNA-based, ribozyme-based and more recently by small-interfering (si)RNA-based and micro (mi)RNA-based, approaches. In particular, RNA interference (RNAi) has great promise for treating dominant diseases in both mutation-dependent and -independent manners, through its efficiency of mRNA transcript cleavage (LaVail et al, 2000; Lewin et al, 1998; O'Reilly et al, 2007; Xia et al, 2004). A possible alternative to such RNA-targeting approaches is the modulation of gene expression at the transcriptional level, by using zinc-finger (ZF)-based artificial transcription factors (ZF-ATFs) that can be tailored to a desired DNA target sequence.

Artificial ZF proteins (ZFPs) are becoming a novel and powerful technological platform for both gene manipulation and development of therapeutics (Jamieson et al, 2003; Pearson, 2008; Segal & Barbas, 2001). ZFPs are composed of a DNA-binding domain (DBD) that is based on the Cys_2His_2 ZF scaffold fused with a transcriptional regulation domain. Their modular structure enables both the sequential assembling of multiple ZFs to generate DBDs with different target specificities and the use of various effector domains to engineer ATFs or nucleases. A single ZF domain consists of approximately 30 amino acids with a simple $\beta\beta\alpha$ fold that is stabilized by hydrophobic interactions and the chelation of a single zinc ion. Each ZF module primarily recognizes an overlapping 4-bp DNA sequence, where the last base pair is the first of the following target (the fourth base of each target is on the opposite strand). The binding takes place through key amino-acid residues, which can be exchanged to generate ZF modules with different sequence specificities. To obtain a DBD that is tailored to a unique target sequence in mammalian genomic DNA (genome size in humans, 3.0×10^9 bp), theoretically, a sequence longer than 16 bp is needed, and this can be achieved by consecutive linking of at least six ZF modules.

To date, several functional ZF-ATFs have been generated to modulate target gene expression *in vitro* (Bartsevich & Juliano, 2000; Beerli et al, 1998; Liu et al, 2001; Zhang et al, 2000); however, none of the *in vivo* studies presented (Mattei et al, 2007; Rebar et al, 2002) have been aimed at silencing a disease gene via vector-mediated somatic-gene transfer.

We designed a two-step repression–replacement strategy (Cashman et al, 2005; Chadderton et al, 2009; Farrar et al, 2002; Gorbatyuk et al, 2005; Kiang et al, 2005; O'Reilly et al, 2007; Xia et al, 2004): (i) mutational-independent silencing of the human rhodopsin (hRHO) gene (transcriptional silencing targeted to both wild-type and mutated RHO alleles); and (ii) gene replacement of the endogenous RHO copies by adeno-associated virus (AAV)-vector-mediated photoreceptor gene transfer. Considering that autosomal dominant *retinitis pigmentosa* (adRP) is the most genetically heterogeneous inherited disease in humans, we designed this mutational-independent strategy to overcome the technical and economical magnitude of allele-specific targeted-designed therapeutics. Indeed, in the case of adRP, due to rhodopsin mutations, more than 150 allele-specific silencing molecules would be required to silence each specific mutation identified thus far (RHO gain-of-function mutations account for 25–50% of the total autosomal dominant adRP cases; (Inglehearn et al, 1998; Sohocki et al, 2001).

Here, we set out to determine whether transcriptional repression by engineered ZFP technology represents a novel therapeutic gene-silencing paradigm for the treatment of gain-of-function mutations. To this end, we used a transgenic mouse model of adRP harbouring a Pro347Ser (P347S) mutation in hRHO.

We show that AAV-vector-mediated photoreceptor delivery of a selected *humanized* ZF artificial transcriptional repressor targeted to the mutated hRHO transgene in P347S adRP mice results in significant reduction of its expression, which in turn leads to improved retinal pathology and function, which validates the first limiting step of the repression–replacement strategy designed.

RESULTS

Design and generation of zinc-finger-based transcription factors to control rhodopsin gene expression

To control RHO expression, we designed ZF-ATFs targeted to the human rhodopsin promoter (hRHO-P). We first scanned the proximal hRHO-P to identify amenable target regions, applying the following criteria: (i) exclusivity of the 18-bp DNA sequences in the human genome; (ii) putative accessibility to the chromatin environment [in proximity to known endogenous transcription-factor binding sites; (Graslund et al, 2005)]; (iii) absence of annotated polymorphisms; and (iv) divergence between the human and murine rhodopsin promoter target sequences. We selected 10 different continuous or discontinuous 18-bp target sites within the proximal region of the hRHO-P (from -90 to -32, relative to the transcription start site; Fig 1a and Table 1) that fulfilled these four criteria. As individual ZFs typically bind 3 or 4 bp of DNA, we generated DBDs by assembling six-ZF arrays that were directed to the selected 18-bp DNA sequences, using the modular assembly method (http://www.zincfingertool.org; Beerli et al, 1998; Mandell & Barbas, 2006; Segal et al, 1999). Due to the lack of availability of ZFs for all possible triplets (Blancafort et al, 2003; Dreier et al, 2001, 2005, 2000; Segal et al, 1999) and to enhanced DNA-binding affinity (Kim & Pabo, 1998), we designed 10 ZF modules with two arms, each composed of three ZF units (arm 1 encoding fingers 1.2.3 and arm 2 encoding fingers 4.5.6) that were bridged together by linker peptides that allowed these ZF modules to span up to 10 bp of DNA gaps between their target-recognition sites (Fig 1b). For gaps longer than 3 bp, we used the structured linker reported by Moore (Moore et al, 2001), whereas for shorter gaps or continuous sequences, we used the flexible linker reported by Rebar (Rebar et al, 2002; Table 1). We next fused the ZF DBDs to a nuclear localization signal, to a C-terminal HA-tag, and to effector domains that included either the herpes simplex virus-based transcriptional activator VP64 domain (Seipel et al, 1992; ZF transcriptional activators; ZF-As) or the human-derived Krüppel-associated box (KRAB) repression domain (Margolin et al, 1994; ZF transcriptional repressors: ZF-Rs; Fig 1b).

In vitro screening of functional ZF-Rs

To select ZF-ATFs that are functional in hRHO-P transcriptional control, we first performed firefly luciferase reporter-gene
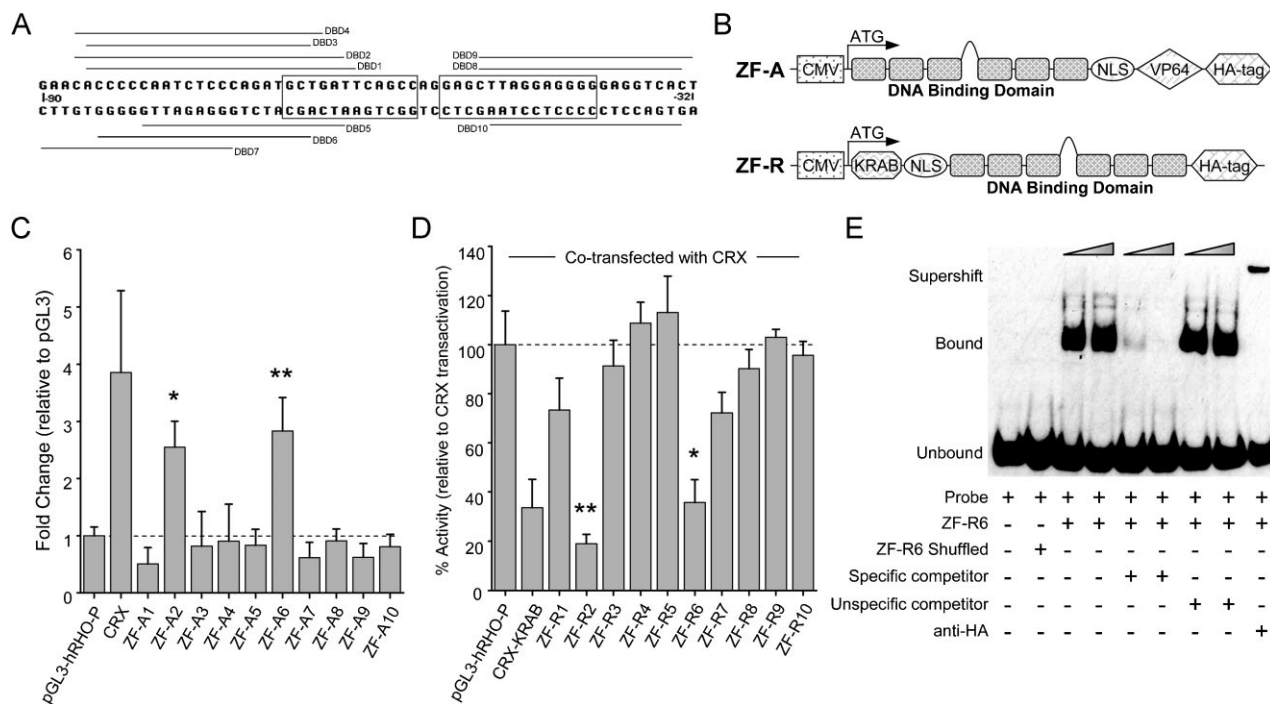
Figure 1. In vitro selection of functional ZF-Rs targeted to the human rhodopsin promoter.

A. DNA sequence of *hRHO* proximal promoter region. Lines, relative positions of DNA sequences targeted by the 10 different DBDs. Boxes, putative binding sites for known endogenous regulators of *hRHO* (Chen & Zack, 1996; Rehemtulla et al, 1996).

B. Schematic representation of the ZF transcriptional activator (ZF-A) and repressor (ZF-R).

C. Histogram showing the fold-changes (luciferase activity relative to the control vector; pGL3-*hRHO*-P) in HEK293 cells upon transfection of the transactivator constructs (ZF-As). ZF-A2 and ZF-A6 significantly transactivated the luciferase expression. As a positive control, pGL3-*hRHO*-P was co-transfected with a plasmid encoding for CRX, a known transactivator of rhodopsin.

D. Histogram showing the extent of repression relative to CRX transactivation of the luciferase activity mediated by ZF-Rs. ZF-R2 and ZF-R6 significantly repressed the luciferase activity induced by CRX. As a positive control CRX DBD was fused to the KRAB repressor domain (CRX-KRAB).

E. Binding activity of ZF-R6 assayed by the electromobility shift assay. Representative sample showing evident shift when increasing amounts of nuclear extract from HEK293 cells transfected with a plasmid coding for the ZF-R6 protein was incubated with the double-stranded specific target site probe (lanes 3 and 4). The shift was not observed using nuclear extract from cells expressing ZF-R6-shuffled (lane 2). Specific binding was abolished upon addition of $10\times$ or $100\times$ molar excess of cold probe to the mix (lanes 5 and 6), whereas no effects can be seen upon addition of $10\times$ or $100\times$ molar excess of an unspecific cold probe (lane 7 and 8). The supershift is obtained by adding an antibody that recognizes the HA-tag of the ZF-R6 in the mix (lane 9).

transactivation assays by co-transfecting HEK293 cells with both the reporter gene driven by the human rhodopsin proximal promoter (-330 to $+32$, relative to the transcription start site) and the individual ZF-A. Two out of the 10 constructs significantly transactivated luciferase expression to levels comparable to those obtained with a plasmid coding for the endogenous rhodopsin transcription activator CRX (cone-rod-homeobox-containing gene) (Chen et al, 1997) (Fig 1c; $n = 5$, from three independent experiments; ZF-A2, $p < 0.01$; ZF-A6, $p < 0.01$). When transfected with a luciferase-expression plasmid containing the murine rhodopsin proximal promoter region (harbouring several mismatches compared to the human counterpart), none of the 10 constructs transactivated the reporter gene expression. The results obtained for the selected functional activators ZF-A2 and ZF-A6 are shown in Figure S1 of Supporting Information. To evaluate ZFP-mediated transcriptional repression, we assessed their down-regulation of CRX-

mediated transcription through triple transfection in HEK293 cells, which included the ZF-Rs, the CRX and the reporter plasmids. Notably, ZF-R2 and ZF-R6, which contain the same DBDs as ZF-A2 and ZF-A6, significantly reduced luciferase expression levels (81 and 64% repression relative to CRX transactivation, respectively; Fig 1d; $n = 5$, from three independent experiments; ZF-R2, $p < 0.001$; ZF-R6, $p < 0.01$), similar to the repression obtained with the CRX DBD fused to KRAB, which was used as the positive control (Chau et al, 2000). As a further control, the activation and repression activities were completely abolished when the relative positions of the six individual ZF units of the DBDs were exchanged (*e.g.* from 1.2.3–4.5.6 to 5.1.6–3.4.2; ZF-A6-shuffled and ZF-R6-shuffled; Figure S2 of Supporting Information). In addition, electromobility shift assays showed binding specificity of ZF-R2 and ZF-R6 to the target promoter sequence *in vitro* (data not shown, and Fig 1e, respectively).

Table 1. Sequences of the binding sites targeted by the artificial transcription factors in the *hRHO* proximal promoter

DBD No	Target DNA sequence (5′–3′)	Gap (bp)	Strand	Linker[a]
1	gaac**ACCCCCAAT**ctcccag**ATGCTGATT**	7	+	A
2	gaa**CACCCCCAA**tctccca**GATGCTGAT**t	7	+	A
3	gaac**ACCCCCAAT**ctc**CCAGATGCT**gatt	3	+	A
4	gaa**CACCCCCAA**tctcc**CAGATGCTG**att	5	+	A
5	cttgtggggg**GTTAGAGGG**t**CTACGACTA**a	1	−	B
6	cttgt**GGGGGTTAG**ag**GGTCTACGA**ctaa	2	−	B
7	**CTTGTGGGGGTTAGAGGG**tctacgactaa	None	−	B
8	**CTTAGGAGG**g**GGAGGTCAC**t	1	+	B
9	**CTTAGGAGG**gg**GAGGTCACT**	2	+	B
10	g**AATCCTCCCCCTCCAGTG**a	None	−	B

DBD, DNA binding domain.

The 18-bp target sequences are highlighted as bold capitals.

[a]Linker A: see Lebherz et al (2008); Linker B: see Farrar et al (2002).

ZF-R-mediated repression of human rhodopsin in retinal stem cells

To probe whether the two selected ZF-ATFs promote rhodopsin transcriptional repression in the chromosomal context, we took advantage of an *in vitro* system to differentiate retinal precursors (retinal stem cells; RSCs (Giordano et al, 2007)). Neurospheres derived from the murine adult ocular ciliary margin can differentiate *in vitro* into various retinal neuronal cell types, including photoreceptor precursors that express rhodopsin, the beta-subunit of phosphodiesterase-6 (*PDE6β*), and the cGMP-gated channel (*Cnga*) (Sanges et al, 2006). We explanted neurospheres from the adult P347S transgenic mouse. This mouse model of adRP harbours a human rhodopsin transcriptional unit (including 4 kb of the proximal rhodopsin promoter region) from a patient carrying a P347S mutation (Li et al, 1996), in addition to the endogenous wild-type murine rhodopsin alleles (mRho). Once differentiated into photoreceptor-like (rhodopsin positive; Rho+) cells, P347S neurospheres underwent apoptosis with kinetics similar to those observed in another severe retinal-degeneration model [the *rd-1* mouse; (Sanges et al, 2006)]. Virtually all of the Rho+ cells were also TUNEL-positive 12 days after adding differentiating medium to the P347S retinal cell precursors (Figure S3 of Supporting Information). Thus, we expected that efficient and specific repression of the human mutated rhodopsin, combined with preservation of the endogenous murine rhodopsin expression, would result in rescue/survival of the photoreceptor precursors. To this end, 7 days after adding the differentiating medium, we transduced P347S retinal precursor cells with retroviruses coding for the selected ZF-Rs (ZF-R2 and ZF-R6) or for ZF-R6-shuffled as a negative control. Twelve days after the induction of differentiation, ∼70% of the cells expressed rhodopsin (*i.e.* were Rho+), 98% of which were also double positive (*i.e.* HA+, Rho+), confirming that retroviruses can transduce retinal cell precursors efficiently (Sanges et al, 2006). ZF-R2 and ZF-R6 transduction produced significant 77 and 92% protection from cell death, respectively, whereas virtually all of the ZF-R6-shuffled transduced cells underwent apoptosis (Fig 2a, b and d; $n = 2$, from two independent experiments; ZF-R2, $p = 4.54 \times 10^{-11}$; ZF-R6, $p = 1.18 \times 10^{-11}$). Confocal images of triple-stained (HA+, Rho+ and TUNEL+) samples confirmed that only cells expressing ZF-R2 or ZF-R6 were protected from apoptosis (Fig 2c).

To determine whether protection from apoptosis was through specific repression of human rhodopsin transcription, we measured *hRHO* mRNA levels 4 days after transduction. Nonetheless, ZF-R2- and ZF-R6-transduced cells showed 51 and 88% reduction, respectively, of the *hRHO* transcript levels, compared to *hRHO* levels in cells treated with ZF-R6-shuffled (Fig 2e; $n = 2$, from two independent experiments; ZF-R2, $p < 0.01$; ZF-R6, $p < 0.01$) after normalization with murine rhodopsin, which was used to discriminate photoreceptor precursor cells (Rho+ cells) from those which were not induced to express rhodopsin. These data show that ZFPs promote *hRHO* transcriptional repression in a chromosomal context and that this, in turn, can protect retinal progenitors of an adRP model from apoptosis.

Delivery of ZF-Rs to murine photoreceptors decreases adRP disease progression

The ZF-R6 construct, which provided robust *hRHO* transcriptional repression and apoptosis protection, was selected for *in vivo* experiments. We generated an AAV2/8 vector, as this is currently considered to be most efficient AAV delivery vehicle for photoreceptor gene transfer (Allocca et al, 2007; Lebherz et al, 2008; Natkunarajah et al, 2008; Stieger et al, 2008). This AAV2/8 vector contained the ZF-R6 construct under the photoreceptor-specific rhodopsin kinase (*RHOK*) promoter element (Allocca et al, 2007) (AAV2/8-RHOK-ZF-R6). In homozygous P347S mice, over-expression of the mutated rhodopsin leads to the fast progression of retinal degeneration. Indeed, by P21, only one row of photoreceptor nuclei was detectable by histology (Figure S4 of Supporting Information). Thus, to decrease human P347S rhodopsin expression levels, we crossed P347S mice with a wild-type C57BL/6 background. The resulting progeny (P347S$^{+/−}$) showed milder retinal degeneration (Figure S4 of Supporting Information). At P70, P347S$^{+/−}$ retinae still retained 5–6 rows of photoreceptor nuclei and residual functionality, thus allowing evaluation of disease progression over time by both histology and electroretinography
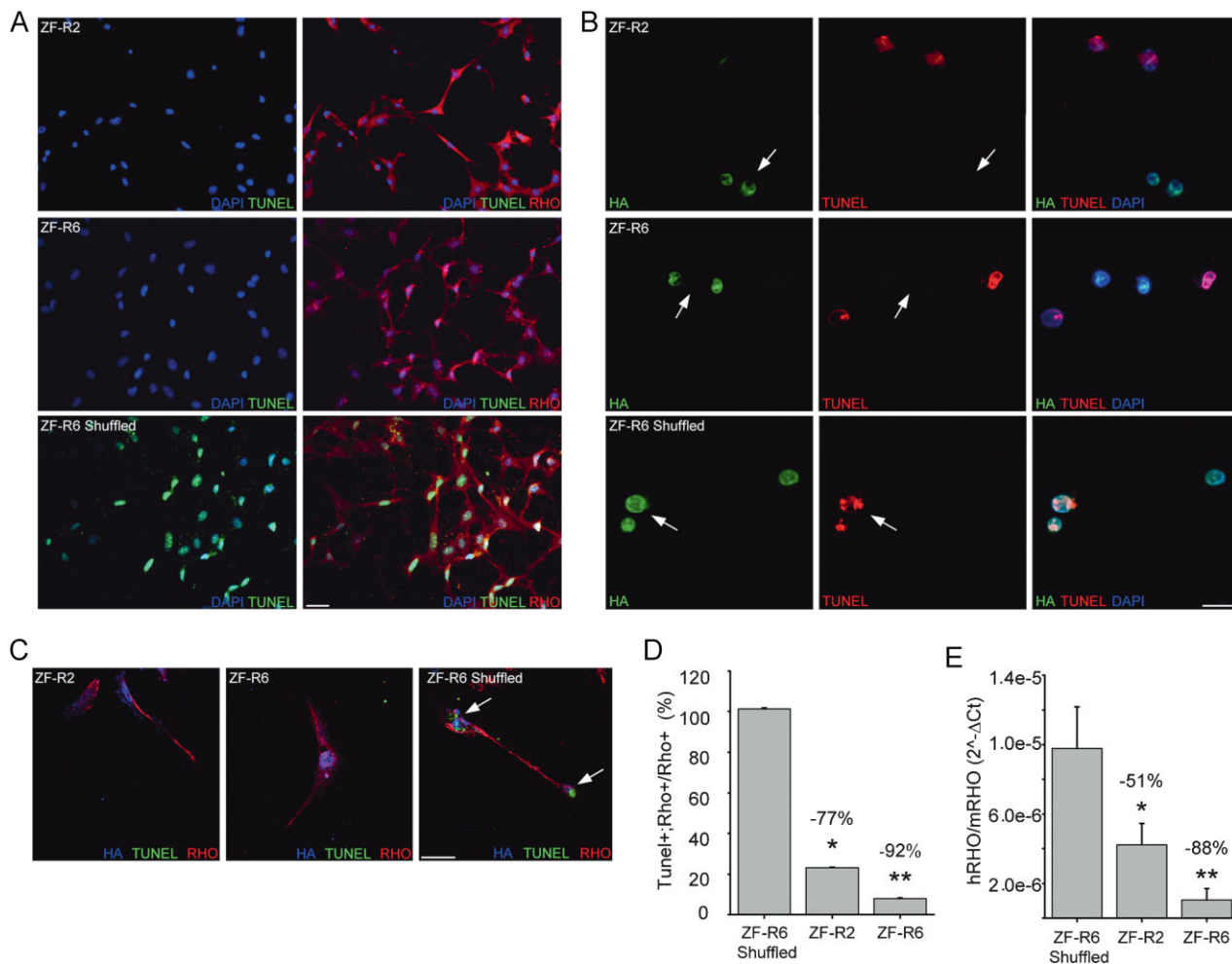
Figure 2. ZFP-mediated repression of rhodopsin in retinal stem cells.

A. Representative rhodopsin and TUNEL staining of RSCs from the P347S mouse following differentiation for 7 days, then transduction with retroviruses containing ZF-R2, ZF-R6 and ZF-R6-shuffled, with analysis after a further 4 days. ZF-R2 and ZF-R6 transduction prevented apoptosis (TUNEL+; green) in Rho+ cells (Red). ZF-R6-shuffled did not protect photoreceptor-like cells from death.

B. Representative immunofluorescence showing the specific protection effects of the ZF-Rs. Photoreceptor-like cells were protected from apoptosis (TUNEL+; red) when transduced (HA+ cells; green) with ZF-R2 and ZF-R6 (arrows). No protection was seen for cells transduced with ZF-R6-shuffled.

C. Representative confocal images showing that Rho+ (red) and HA+ (blue) cells are protected from apoptosis (TUNEL+; green) only when transduced with ZF-R2 and ZF-R6.

D. Histogram showing quantification of the data reported in (A).

E. Histogram from quantitative RT-PCR analysis of *hRHO* mRNA levels in transduced cells. The values were normalized with photoreceptor-specific mRho transcript levels, which were used as a marker to normalize the number of photoreceptor precursor cells from those that were not induced to express rhodopsin and were dying at the time of analysis. $^*p < 0.01$; $^{**}p < 0.001$, as statistically significance differences (*t*-test).

(ERG) analysis. We first assessed transcriptional repression by subretinal co-injection in P4 P347S$^{+/-}$ of 1×10^9 genome copies (GC) of AAV2/8-RHOK-ZF-R6 and a vector coding for the enhanced green fluorescent protein (EGFP; AAV2/1-CMV-EGFP), to identify the transduced retinal area. The contralateral eye received a mix of AAV2/1-CMV-EGFP and AAV2/8-RHOK-EGFP vectors as control. Western blotting showed expression of the ZF-R6 protein in the retina 12 days post-injection (P18, before photoreceptor degeneration; Fig 3a). Quantitative real-time polymerase chain reaction (PCR) analysis demonstrated that the EGFP-positive portion of the retinae treated with AAV2/

8-RHOK-ZF-R6 showed significant, ~26%, reduction in the *hRHO* transcript levels relative to the endogenous mRho, compared to the contralateral EGFP-treated retinae (Fig 3b; *n* = 9, from two independent littermates; *p* < 0.01). In contrast, the expression profiles of three photoreceptor-specific genes were unchanged (Fig 3b; *n* = 4).

We next evaluated the ability of AAV2/8-RHOK-ZF-R6 to impact on P347S photoreceptor disease progression. As we noted that there was variability in the retinal function assessed by recording the electrophysiological response of the retina to increasing light intensities (ERG) among different littermates,
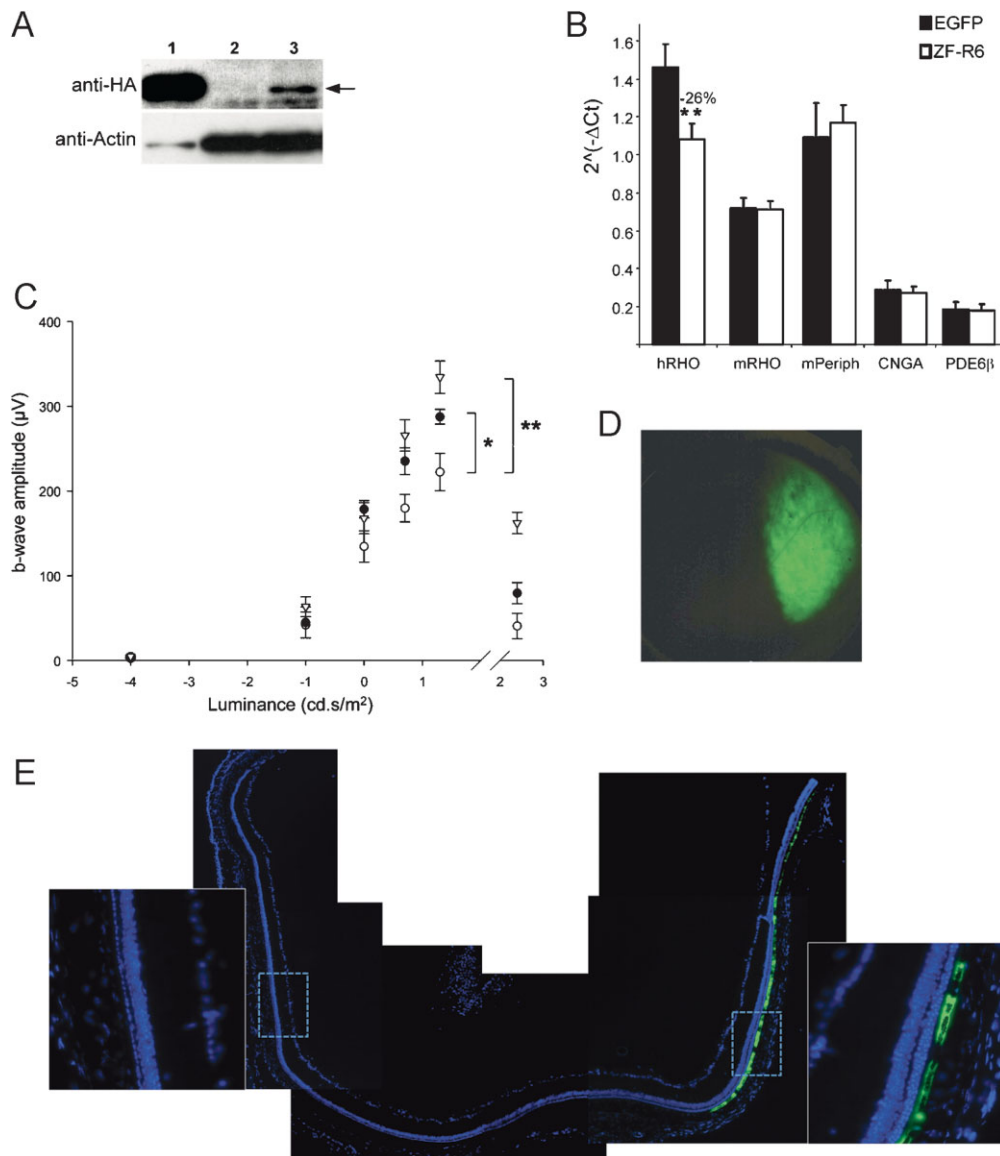
Figure 3. AAV-mediated photoreceptor ZFP gene transfer reduces the severity of adRP retinal dystrophy.

A. Representative Western blot with an anti-HA antibody of the lysates from P347S retinae (P18) injected with AAV2/8-RHOK-ZF-R6 at P4. Lane 1: HEK293 cells transfected with a plasmid encoding for ZF-R6; lane 2: P347S retinal extracts transduced with AAV2/1-CMV-EGFP and AAV2/8-RHOK-EGFP; lane 3: P347S retinal extracts transduced with AAV2/8-RHOK-ZF-R6 and AAV2/1-CMV-EGFP. Actin expression was used for normalization (anti-actin antibody).

B. Histogram from quantitative RT-PCR analysis on P18 retinae transduced at P4 with AAV2/8-RHOK-ZF-R6 and AAV2/1-CMV-EGFP. Specific down-regulation, by 26%, of human rhodopsin transgene expression was measured in the treated eyes (white bars) compared to the control-injected eyes (black bars). Photoreceptor specific gene expression levels (*murine rhodopsin, peripherin, PDE6β* and *Cnga*) remained unaltered in treated and control retinae (values normalized *versus* endogenous GAPDH transcript levels). $^{**}p < 0.05$, as statistically significance difference between ZF-R6 and EGFP treated eyes of the same animals (*t*-test).

C. Electrophysiological responses of retina recorded by ERG analysis, on P347S$^{+/-}$ mice injected subretinally with AAV2/8-RHOK-ZF-R6 and AAV2/1-CMV-EGFP or AAV2/1-CMV-EGFP and AAV2/8-RHOK-EGFP at P30. The amplitudes represent retinal responses evoked by increasing light intensities under scotopic (dim light) and photopic (bright light) conditions. B-wave amplitudes before treatment (base-line: P30; open triangles, $n = 34$ eyes, 17 animals) and after treatment (P90; filled circles, $n = 16$ eyes, AAV2/8-RHOK-ZF-R6 treated animals; open circles, $n = 15$ eyes, AAV2/8-RHOK-EGFP treated animals). Sixty days after vector delivery, the electrophysiologic responses of the retina were preserved in ZF-R6-treated eyes (black circles) compared to control contralateral EGFP injected eyes (open circles). $^{*}p < 0.01$; $^{**}p < 0.001$, as statistically significance differences between EGFP control eyes (P90) and base-line responses (P30).

D. Representative indirect ophthalmoscopy of retinal fundus. Fluorescent EGFP expression indicates the extension of retinal exposure after AAV vector administration (P90 P347S retina co-injected with AAV2/8-RHOK-ZF-R6 and AAV2/8-RHOK-EGFP).

E. Representative immunofluorescence histological analysis of AAV2/8-RHOK-ZF-R6 treated retina showing the EGFP-positive retinal portion transduced (right; dotted square, selected field at higher magnification, 20×; co-injection of AAV2/8-RHOK-ZF-R6 and AAV2/8-RHOK-EGFP). This treatment resulted in partial preservation of photoreceptor cell nuclei, as compared to EGFP-negative area (left; dotted square as before).

and despite similar P347S rhodopsin levels, we decided to contextually measure base-line ERG parameters and treat the animals subretinally. We performed subretinal injections of 1×10^9 GC of AAV2/8-RHOK-ZF-R6 in three independent 1-month-old P347S$^{+/-}$ littermates (P30; for a total of 17 animals, 34 eyes: 17 RHOK-ZF-R6 and 17 RHOK-EGFP eyes), with the paired eye of the same animals receiving the same vector dose of AAV2/8-RHOK-EGFP. At 60 days following this subretinal vector administration (P90), the eyes that received AAV2/8-RHOK-ZF-R6 showed preservation of ERG responses, as compared to the control EGFP-treated eyes of the same animals, in which the degeneration led to a ∼40% reduction in the b-wave maximum amplitude (Table 1 of Supporting Information, Fig 3c). In addition, histological analysis of mice at P90–100 demonstrated that the ZF-R6-transduced portion of the retina (typically 30–50% of the retina, Fig 3e), was associated with partial protection of the photoreceptor degeneration in seven eyes out of the nine analysed (Fig 3d and e).

Finally, to evaluate potential toxicity on retinal function of a healthy mouse retina due to ZF-R6 treatment, we injected AAV2/8-RHOK-ZF-R6 subretinally in a cohort of 10 C57BL/6 animals. Two months after vector delivery, no histological abnormalities or reductions in either the a-waves or b-waves were seen for the treated eyes, as compared to untreated parental eyes, thus supporting the safety of this approach (Figure S5 of Supporting Information).

DISCUSSION

In the present study, we have demonstrated that photoreceptor delivery of an AAV2/8 vector containing artificial ZF transcriptional repressors (ZF-R6) targeted to the *hRHO* promoter can repress *hRHO* transgene over-expression, and this, in turn, was associated with improvement in photoreceptor disease in the P347S mouse model of adRP. Our findings extend the possible uses of artificial ZF-based DBPs as novel therapeutics for the treatment of dominant diseases.

A different technological platform based on RNAi was first used *in vivo* to silence a dominant allele of ataxin-1 for the treatment of spinocerebellar ataxia type 1 in a mutational-independent manner; this approach was then applied to other mouse models of human disease, including the P347S adRP mouse (O'Reilly et al, 2007; Xia et al, 2004). Thus, based on the data presented here, transcriptional (artificial ZFP technology) or post-transcriptional (RNAi) silencing strategies can be considered as alternatives to one another; however, in the light of the different molecular mechanisms underlying these two silencing strategies (promoter binding and transcription inhibition of ZF *vs.* enzyme-like degradation of mRNA by RNAi), a side-by-side comparison will be necessary to determine which of these two systems is the safest and the most efficacious. Moreover, as well as the off-target silencing events that will potentially set the hurdles for the development of a safe ZFP-based or RNAi-based system, studies have shown that high levels of siRNAs can cause cellular toxicity through various mechanisms (Boudreau et al, 2009; Grimm et al, 2006). Also, an attractive and therapeutically valuable feature of ZFPs is the possibility to control their expression levels through the use of inducible promoter systems, which have not yet been optimized for the control of RNAi-based repression systems. Indeed, a key safety and efficacy element for the success of silencing strategies relies on the fine-tuning control of the expression levels of the repressor system.

The transcriptional, mutational-independent strategy used in the present study is aimed at overcoming the heterogeneity of mutations in the *RHO* gene. Indeed, the design of mutation-specific silencing molecules is technically, and economically, particularly challenging, considering that: (i) retinitis pigmentosa is widely thought to be the most genetically heterogeneous disorder in man (Wright et al, 2010); and (ii) over 150 dominant mutations in rhodopsin are known to date (OMIN database 180380). As has been previously suggested (*e.g.* RNAi-mediated suppression and replacement of human rhodopsin *in vivo*; (O'Reilly et al, 2007), we propose here to apply a general strategy that is based on the repression of both the mutated and the wild-type alleles, and the simultaneous replacement of the endogenous gene copies with the exogenous vector-delivered gene [repression–replacement strategy; (O'Reilly et al, 2007)]. In the present study, the ZF-Rs acted as transcriptional *hRHO*-specific silencers, whereas the endogenous copies of murine Rho alleles functioned as a replacement gene. Thus, one future development should be the use of an amenable mouse model (ideally harbouring both a mutated and a normal *hRHO* gene on a *mRho*-knock-out background) to determine whether down-regulation of both alleles together with simultaneous replacement with a *hRHO* transgene (under the transcriptional control of a promoter insensitive to the ZF-R) will result in phenotypic rescue. Although this needs to be tested, the feasibility of this proposed approach is based on the following considerations: (i) we have demonstrated the ability to down-regulate the levels of transcription somatically (via AAV-vector delivery), which represents the major limiting step in the strategy; (ii) the therapeutic levels of transcriptional silencing result in phenotype amelioration (26%), and thereby the levels of RHO necessary for replacement appear feasible to achieve, considering the proof-of-concept obtained with the gene-replacement approach in different animal models of retinal degeneration [recently also in *Rho*$^{-/-}$ mice; (Chadderton et al, 2009)], as well as clinical trials (Bainbridge et al, 2008; Hauswirth et al, 2008; Maguire et al, 2008); and (iii) there is the possibility to incorporate two genes into the same vector (both the silencing and the replacement constructs in our case), as this has been demonstrated in AAV vectors by us and others (Allocca et al, 2007; Nguyen et al, 2007). Indeed, a vector that incorporates both the artificial ZF-based repressor and the replacement gene will ensure their simultaneous and balanced silencing and repression action in the same transduced photoreceptors [*e.g.* with bidirectional promoters allowing the coordinated expression of the two transgenes; (Amendola et al, 2005)]. Moreover, it has been shown that both high and low rhodopsin expression levels can be deleterious to rod function, which suggests that tight regulation of rhodopsin expression levels is required for the successful application of any retinal repression–replacement strategy.

Finally, the versatility of ZFP design theoretically allows to switch the repressor with an activator domain (maintaining the same DBD) to also treat dominant diseases that are due to haploinsufficiency.

The results from the present study demonstrate that the novel and generally applicable mutational-independent strategy based on artificial ZFPs allows transcriptional control of an endogenous causative gene and has therapeutic relevance for the treatment of diseases due to gain-of-function mutations.

MATERIALS AND METHODS

Rational design of zinc-finger-based artificial transcription factors

DBDs targeted to 10 different target sites in the *hRHO* promoter (Table 1) were obtained using the web-based Zinc Finger Tools [http://www.zincfingertools.org; (Mandell & Barbas, 2006)]. These were composed of two arms, each of which recognized a 9-bp half-target site, and they were fused together through a linker sequence, to bridge the gap sequence. We used two different linkers according to the lengths of the gaps: for gaps longer than 3 bp (target sites from 1 to 4), we used a complex structured linker, as reported by Moore [(Moore et al, 2001); GRSSVESACVTSVLVALLPATSAPTQVSG], while for longer gaps (target sites from 5 to 10), we used a flexible linker, as described by Rebar [(Rebar et al, 2002); QNKKGGSGDGKKKQHI]. We optimized the corresponding DNA sequences to facilitate the subsequent cloning steps, and purchased these as transgenes in the pLS-standard vector (TOP Gene Technologies, Quebec, Canada). After the *in vitro* selection steps, we purchased an additional DBD with the fingers of DBD number six shuffled (from 1.2.3–4.5.6 to 5.1.6–3.4.2) to be used as a negative control for a total of 11 DBDs. All of the DBDs were flanked by a ClaI and an XbaI site at the 5′ and 3′ ends, respectively.

DBD number 1 was purchased as a complete protein fused at the N-terminal with the repressor domain KRAB (Krüppel-associated box, DAKSLTAWSRTLVTFKDVFVDFTREEWKLLDTAQQILYRNVMLENYKNLVSL-GYQLTKPDVILRLEKGEEPWLVEREIHQETHPDSETAFEIKSSV) and the nuclear localization signal (PKKKRKV) from the SV40 large T antigen, and fused at the C-terminal with the HA-tag (YPYDVPDYAS). Also, DBD number 2 was purchased as a complete protein, but fused at the C-terminal with the nuclear localization signal, the activator domain VP64 (tetrameric repeat of herpes simplex VP16 minimal-activation domain, GRADALDDFDLDMLGSDALDDFDLDMLGSDALDDFDLDMLGS-DALDDFDLDMLIN) and the HA-tag. In the two proteins, the DBDs can be exchanged through a double digestion with the restriction endonucleases ClaI and XbaI.

The 11 different transcription activators (ZF-As) and repressors (ZF-Rs) were inserted in the pAAV2.1-CMV-EGFP NotI and HindIII sites, downstream of the cytomegalovirus (CMV) promoter, by removing the EGFP coding sequence for transfection experiments. For AAV preparations, ZF-R6 was inserted in the pAAV2.1-RK-EGFP NotI and HindIII sites, downstream of the RHOK promoter, by removing the EGFP coding sequence. For retrovirus preparations used in RSC experiments, coding sequences of ZF-R2, ZF-R6 and ZF-R6-shuffled were cloned in the LXSN plasmid EcoRI and HindIII sites downstream of the CMV promoter.

Reporter constructs

Luciferase reporter plasmids were generated from the pGL3-Basic vector (Promega, Madison, WI, USA), by cloning the proximal upstream regions of the human or murine rhodopsin gene (see Materials and Methods Section of Supporting Information).

Screening of the functional ZF-ATFs in human cells by transient transfection

HEK293 cells were plated in six-well plates at a density of 400,000 cells/well. Twenty-four hours later, the cells were co-transfected using FUGENE 6 (Roche, Basel, Switzerland), following the manufacturer instructions. Transfection cocktails included 200 ng reporter plasmid (or pGL3basic as a negative control), 300 ng ZF-ATF, 300 ng of a plasmid encoding for murine CRX (alone, as a positive control in transactivation assays, or in combination with the ZF-Rs, for repression assays) and 10 ng *Renilla* luciferase reporter plasmid control (Promega), to normalize for transfection efficiency. The amount of DNA was kept constant by adding pAAV2.1-TBG-EGFP, to a total of 1 μg. Cells were harvested 48 h after transfection in 1× PLB Lysis Buffer (Promega). Firefly and *Renilla* luciferase activities were measured in a GloMax^{TM} luminometer (Promega), using the Dual Luciferase Reporter Assay System (Promega).

Electromobility shift assay

Electromobility shift assays were performed using Lightshift Chemi-luminescent Electromobility Shift Assay kits (Pierce), following the manufacturer instructions. The detailed procedure is available in the Materials and Methods Section of Supporting Information.

AAV vector production and purification

AAV vectors were produced by the TIGEM AAV Vector Core using pAAV2.1-RK-ZF-R6 and pAAV2.1-CMV-EGFP. Recombinant AAV8 viruses were produced by triple transfection of HEK293 cells followed by CsCl$_2$ purification of the vectors, as previously described (Auricchio et al, 2001). For each viral preparation, physical titers (GC/ml) were determined by both PCR quantification using TaqMan (Perkin-Elmer, Life and Analytical Sciences, Inc.) and by dot-blot analysis.

RNA preparation and measurement of rhodopsin transcript levels by real-time PCR

RNAs from tissues and cells were isolated using TRIZOL reagent (Invitrogen), according to the manufacturer protocol. cDNA was amplified from 500 ng isolated RNA using SuperScript^{TM} III First-Strand Synthesis (Invitrogen), as indicated in the manufacturer instructions. Transcript levels of human and murine rhodopsin were measured by real-time PCR using the ABI Prism 7000 Sequence Detection System (Applied Biosystems, Foster City, CA, USA) and the following primers: hRho_forward 5′...CCGGCTGGTCCAGGTACAT...3′ and hRho_reverse 5′...TTGTTGACCTCCGGCTTGAG...3′; mRho_forward 5′...TGTTGAACAAGCAGTTCCGGA...3′ and mRho_reverse 5′...TCGTCATCTCCCAGTGGATTC...3′. The PCRs with cDNA were carried out in a total volume of 25 μl, using 12.5 μl SYBR Green Master Mix (Applied Biosystems) and 400 nM primers under the following conditions: preheating, 50°C for 2 min, and 95°C for 10 min; cycling, 40 cycles of 95°C for 15 s and 60°C for 1 min. All of the reactions were standardized against murine GAPDH using the following primers: mGAPDH_forward 5-′...CTTCACCACCATGGAGAAGGC...-3′ and

The paper explained

PROBLEM:

Autosomal dominant forms of Retinitis Pigmentosa (adRP) are incurable progressive inherited retinal degenerations, which inexorably lead to blindness. The major hurdles to design effective therapeutic strategies for these diseases are: the genetic heterogeneity (a number of distinct mutations affect numerous individual gene), and the tools to turn off mutated genes are inefficient and difficult to be delivered specifically and efficiently to diseased cells.

RESULTS:

We generated artificial zinc-finger transcriptional repressors (ZFRs) capable to bind DNA regulatory regions controlling rhodopsin gene (RHO) expression, one of the most frequently genes mutated in adRP. To overcome genetic heterogeneity we designed ZFRs that silence RHO in a mutational-independent fashion. We showed that adeno-associated (AAV) viral vector-mediated delivery of ZFR to photoreceptors of a mouse model of adRP that carries a dominant RHO mutation, result in robust down-regulation of RHO and that this in turn results in improvement of disease progression.

IMPACT:

Our results are the first to demonstrate that ZF technology can be exploited to induce transcriptional gene silencing of an endogenous gene via viral vector-mediated delivery *in vivo*. This proof-of-concept study holds promise for the development of novel therapeutics for adRP-associated with any rhodopsin mutation and a variety of other inherited disorders.

---

mGAPDH_reverse 5′-…CTCATGACCACAGTCCATGCC…-3′. To quantify expression levels of photoreceptor specific genes (*Peripherin*, *PDE6β* and *Cnga*) we used the following primers: for *Peripherin*: mPeriph.forward 5′-CGGGACTGGTTCGAGATTC-3′ and mPeriph.reverse 5′-ATC-CACGTTGCTCTTGATGC-3′; for *PDE6β*: PDE6β.forward 5′-TGAAGATGAAGATGTTTTCACG-3′ and PDE6β.reverse 5′-CTCTGCGTGTCTCACAGTTG-3′; for *Cnga*: Cnga.forward 5′-ACTCGTA-CAAAAGGCGAGGAC-3′ and Cnga.reverse 5′-CTTTGTTGCTGCTGTTGTTGAC-3′. Each sample was analysed in triplicate in two-independent experiments.

Retinal stem cell culture and analysis

All procedures on mice (including their euthanasia) were performed in accordance with the ARVO Statement for the Use of Animals in Ophthalmic and Vision Research, and with institutional guidelines for animal research.

RSCs were isolated from adult P347S mice and incubated for 5 days, until floating spheres formed in the serum-free medium (DMEM-F12 with 0.6% glucose and N2 hormone mix) containing 20 ng/ml basic FGF supplemented with 2 μg/ml heparin (Sigma, Milan, Italy), as previously described (Sanges et al, 2006). The retinal floating spheres were allowed to differentiate in DMEM-F12 supplemented with 1% foetal bovine serum (Gibco, San Giuliano Milanese, Italy), in eight-well glass slides that were coated with extracellular matrix (Sigma). The analysis was performed 12 days after induction of differentiation. Apoptotic nuclei were revealed using the TdT-dUTP terminal nick-end labelling kit (TUNEL, Roche Diagnostics, Monza, Italy), according to the manufacturer protocol. For immunofluorescence staining of RSCs, see Materials and Methods Section of Supporting Information.

Animal model, vector administration and tissue collection

All procedures were performed in accordance with institutional guidelines for animal research and all of the animal studies were approved by the authors. P347S$^{+/+}$ animals for breeding were kindly provided by Dr. G. Jane Farrar (Smurfit Institute of Genetics, Trinity College Dublin, Dublin, Ireland) and were bred in the animal facility of the Biotechnology Centre of the Cardarelli Hospital (Naples, Italy) with C57BL/6 mice (Charles Rivers Laboratories, Calco, Italy), to obtain the P347S$^{+/-}$ mice. At P4, the animals were anesthetized on ice and injected subretinally in the right eye with 1 μl AAV2/8-RHOK-ZF-R6 vector (6.3×10^{12} GC/ml) and 1 μl of AAV2/1-CMV-EGFP (6.0×10^{12} GC/ml) in a mixture, whereas the contralateral (control) eye received the same dose of AAV2/1-CMV-EGFP and AAV2/8-RHOK-EGFP vectors as a mixture. The mice were sacrificed at post-natal day 18 or at 1 month of age (P18 or P30). For morphological studies, the eyecups were harvested, fixed by immersion in 4% paraformaldehyde, and then embedded in OCT (Kaltek) The detailed procedures for the histological analysis are given in the Materials and Methods Section of Supporting Information. For RNA extractions, the isolated retinae were removed and snap-frozen in liquid nitrogen, and then treated as described in the above RNA preparation section.

Indirect ophthalmoscopy

The mice were anesthetized with avertin, and their pupils were dilated with topically applied 1% tropicamide. Indirect ophthalmoscopy was performed using a 90-diopter lens. Photographs were taken with a Kowa Genesis camera (Keeler Instruments, Broomall, PA, USA).

Electroretinogram measurements

ERGs were performed at P30, P70 and P90. The detailed procedures are given in the Materials and Methods Section of Supporting Information. Amplitudes of the a-waves and b-waves were plotted as functions of increasing light intensities.

Statistics

The data are expressed as means ± standard error of the mean (s.e.m.), as indicated, and compared by two-tailed Student's *t*-tests, and two-sample equal variance.

Author contributions

The overall study was conceived and designed by CM and EMS, with important contributions from DS, CB, VM, AA and GM. CM, DS, EM, CB and EMS: performed the experiments. CM, DS, EM, UD, AA, GM and EMS: analysed the data. AA and VM: contributed reagents or analysis tools. EMS wrote the paper with substantial contribution from CM.

For more information

Zinc Finger technology:

The Zinc Finger Tool
http://www.scripps.edu/mb/barbas/zfdesign/zfdesignhome.php

The Zinc Finger Consortium
http://www.zincfingers.org/default2.htm

Retinitis Pigmentosa:

Online Mendelian Inheritance in Man (OMIM)
http://www.ncbi.nlm.nih.gov/omim/268000
http://www.ncbi.nlm.nih.gov/omim/180380

Retinal Information Network database
http://www.sph.uth.tmc.edu/Retnet/

Retinal International
http://www.retina-international.org/

European Vision Research
http://www.vision-research.eu/

Foundation Fighting Blindness
http://www.blindness.org/

The Vision of Children Foundation
http://www.visionofchildren.org/

Author's website:
http://www.tigem.it/researchers/enrico-maria-surace

References

Aiuti A, Cattaneo F, Galimberti S, Benninghoff U, Cassani B, Callegaro L, Scaramuzza S, Andolfi G, Mirolo M, Brigida I, *et al* (2009) Gene therapy for immunodeficiency due to adenosine deaminase deficiency. N Engl J Med 360: 447-458

Allocca M, Mussolino C, Garcia-Hoyos M, Sanges D, Iodice C, Petrillo M, Vandenberghe LH, Wilson JM, Marigo V, Surace EM, *et al* (2007) Novel adeno-associated virus serotypes efficiently transduce murine photoreceptors. J Virol 81: 11372-11380

Amendola M, Venneri MA, Biffi A, Vigna E, Naldini L (2005) Coordinate dual-gene transgenesis by lentiviral vectors carrying synthetic bidirectional promoters. Nat Biotechnol 23: 108-116

Auricchio A, Kobinger G, Anand V, Hildinger M, O'Connor E, Maguire AM, Wilson JM, Bennett J (2001) Exchange of surface proteins impacts on viral vector cellular specificity and transduction characteristics: the retina as a model. Hum Mol Genet 10: 3075-3081

Bainbridge JW, Smith AJ, Barker SS, Robbie S, Henderson R, Balaggan K, Viswanathan A, Holder GE, Stockman A, Tyler N, *et al* (2008) Effect of gene therapy on visual function in Leber's congenital amaurosis. N Engl J Med 358: 2231-2239

Bartsevich VV, Juliano RL (2000) Regulation of the MDR1 gene by transcriptional repressors selected using peptide combinatorial libraries. Mol Pharmacol 58: 1-10

Beerli RR, Segal DJ, Dreier B, Barbas CF III (1998) Toward controlling gene expression at will: specific regulation of the erbB-2/HER-2 promoter by using polydactyl zinc finger proteins constructed from modular building blocks. Proc Natl Acad Sci USA 95: 14628-14633

Blancafort P, Magnenat L, Barbas CF III (2003) Scanning the human genome with combinatorial transcription factor libraries. Nat Biotechnol 21: 269-274

Boudreau RL, Martins I, Davidson BL (2009) Artificial microRNAs as siRNA shuttles: improved safety as compared to shRNAs *in vitro* and *in vivo*. Mol Ther 17: 169-175

Cartier N, Hacein-Bey-Abina S, Bartholomae CC, Veres G, Schmidt M, Kutschera I, Vidaud M, Abel U, Dal-Cortivo L, Caccavelli L, *et al* (2009) Hematopoietic stem cell gene therapy with a lentiviral vector in X-linked adrenoleukodystrophy. Science 326: 818-823

Cashman SM, Binkley EA, Kumar-Singh R (2005) Towards mutation-independent silencing of genes involved in retinal degeneration by RNA interference. Gene Ther 12: 1223-1228

Chadderton N, Millington-Ward S, Palfi A, O'Reilly M, Tuohy G, Humphries MM, Li T, Humphries P, Kenna PF, Farrar GJ (2009) Improved retinal function in a mouse model of dominant retinitis pigmentosa following AAV-delivered gene therapy. Mol Ther 17: 593-599

Chau KY, Chen S, Zack DJ, Ono SJ (2000) Functional domains of the cone-rod homeobox (CRX) transcription factor. J Biol Chem 275: 37264-37270

Chen S, Zack DJ (1996) Ret 4, a positive acting rhodopsin regulatory element identified using a bovine retina *in vitro* transcription system. J Biol Chem 271: 28549-28557

Chen S, Wang QL, Nie Z, Sun H, Lennon G, Copeland NG, Gilbert DJ, Jenkins NA, Zack DJ (1997) Crx, a novel Otx-like paired-homeodomain protein, binds to and transactivates photoreceptor cell-specific genes. Neuron 19: 1017-1030

Dreier B, Segal DJ, Barbas CF, III (2000) Insights into the molecular recognition of the 5′-GNN-3′ family of DNA sequences by zinc finger domains. J Mol Biol 303: 489-502

Dreier B, Beerli RR, Segal DJ, Flippin JD, Barbas CF, III (2001) Development of zinc finger domains for recognition of the 5′-ANN-3′ family of DNA sequences and their use in the construction of artificial transcription factors. J Biol Chem 276: 29466-29478

Dreier B, Fuller RP, Segal DJ, Lund CV, Blancafort P, Huber A, Koksch B, Barbas CF, III (2005) Development of zinc finger domains for recognition of the 5′-CNN-3′ family DNA sequences and their use in the construction of artificial transcription factors. J Biol Chem 280: 35588-35597

Farrar GJ, Kenna PF, Humphries P (2002) On the genetics of retinitis pigmentosa and on mutation-independent approaches to therapeutic intervention. EMBO J 21: 857-864

Giordano F, De Marzo A, Vetrini F, Marigo V (2007) Fibroblast growth factor and epidermal growth factor differently affect differentiation of murine retinal stem cells *in vitro*. Mol Vis 13: 1842-1850

Gorbatyuk MS, Pang JJ, Thomas J, Jr, Hauswirth WW, Lewin AS (2005) Knockdown of wild-type mouse rhodopsin using an AAV vectored ribozyme as part of an RNA replacement approach. Mol Vis 11: 648-656

Graslund T, Li X, Magnenat L, Popkov M, Barbas CF, III (2005) Exploring strategies for the design of artificial transcription factors: targeting sites proximal to known regulatory regions for the induction of gamma-globin expression and the treatment of sickle cell disease. J Biol Chem 280: 3707-3714

Grimm D, Streetz KL, Jopling CL, Storm TA, Pandey K, Davis CR, Marion P, Salazar F, Kay MA (2006) Fatality in mice due to oversaturation of cellular microRNA/short hairpin RNA pathways. Nature 441: 537-541

Hauswirth WW, Aleman TS, Kaushal S, Cideciyan AV, Schwartz SB, Wang L, Conlon TJ, Boye SL, Flotte TR, Byrne BJ, et al (2008) Treatment of leber congenital amaurosis due to RPE65 mutations by ocular subretinal injection of adeno-associated virus gene vector: short-term results of a phase I trial. Hum Gene Ther 19: 979-990

Inglehearn CF, Tarttelin EE, Plant C, Peacock RE, al-Maghtheh M, Vithana E, Bird AC, Bhattacharya SS (1998) A linkage survey of 20 dominant retinitis pigmentosa families: frequencies of the nine known loci and evidence for further heterogeneity. J Med Genet 35: 1-5

Jamieson AC, Miller JC, Pabo CO (2003) Drug discovery with engineered zinc-finger proteins. Nat Rev Drug Discov 2: 361-368

Kaplitt MG, Feigin A, Tang C, Fitzsimons HL, Mattis P, Lawlor PA, Bland RJ, Young D, Strybing K, Eidelberg D, et al (2007) Safety and tolerability of gene therapy with an adeno-associated virus (AAV) borne GAD gene for Parkinson's disease: an open label, phase I trial. Lancet 369: 2097-2105

Kiang AS, Palfi A, Ader M, Kenna PF, Millington-Ward S, Clark G, Kennan A, O'Reilly M, Tam LC, Aherne A, et al (2005) Toward a gene therapy for dominant disease: validation of an RNA interference-based mutation-independent approach. Mol Ther 12: 555-561

Kim JS, Pabo CO (1998) Getting a handhold on DNA: design of poly-zinc finger proteins with femtomolar dissociation constants. Proc Natl Acad Sci USA 95: 2812-2817

LaVail MM, Yasumura D, Matthes MT, Drenser KA, Flannery JG, Lewin AS, Hauswirth WW (2000) Ribozyme rescue of photoreceptor cells in P23H transgenic rats: long-term survival and late-stage therapy. Proc Natl Acad Sci USA 97: 11488-11493

Lebherz C, Maguire A, Tang W, Bennett J, Wilson JM (2008) Novel AAV serotypes for improved ocular gene transfer. J Gene Med 10: 375-382

Lewin AS, Drenser KA, Hauswirth WW, Nishikawa S, Yasumura D, Flannery JG, LaVail MM (1998) Ribozyme rescue of photoreceptor cells in a transgenic rat model of autosomal dominant retinitis pigmentosa. Nat Med 4: 967-971

Li T, Snyder WK, Olsson JE, Dryja TP (1996) Transgenic mice carrying the dominant rhodopsin mutation P347S: evidence for defective vectorial transport of rhodopsin to the outer segments. Proc Natl Acad Sci USA 93: 14176-14181

Liu PQ, Rebar EJ, Zhang L, Liu Q, Jamieson AC, Liang Y, Qi H, Li PX, Chen B, Mendel MC, et al (2001) Regulation of an endogenous locus using a panel of designed zinc finger proteins targeted to accessible chromatin regions. Activation of vascular endothelial growth factor A. J Biol Chem 276: 11323-11334

Maguire AM, Simonelli F, Pierce EA, Pugh EN, Jr, Mingozzi F, Bennicelli J, Banfi S, Marshall KA, Testa F, Surace EM, et al (2008) Safety and efficacy of gene transfer for Leber's congenital amaurosis. N Engl J Med 358: 2240-2248

Maguire AM, High KA, Auricchio A, Wright JF, Pierce EA, Testa F, Mingozzi F, Bennicelli JL, Ying GS, Rossi S, et al (2009) Age-dependent effects of RPE65 gene therapy for Leber's congenital amaurosis: a phase 1 dose-escalation trial. Lancet 374: 1597-1605

Mandell JG, Barbas CF, III (2006) Zinc Finger Tools: custom DNA-binding domains for transcription factors and nucleases. Nucleic Acids Res 34: W516-W523

Margolin JF, Friedman JR, Meyer WK, Vissing H, Thiesen HJ, Rauscher FJ, III (1994) Kruppel-associated boxes are potent transcriptional repression domains. Proc Natl Acad Sci USA 91: 4509-4513

Mattei E, Corbi N, Di Certo MG, Strimpakos G, Severini C, Onori A, Desantis A, Libri V, Buontempo S, Floridi A, et al (2007) Utrophin up-regulation by an artificial transcription factor in transgenic mice. PLoS One 2: e774

Moore M, Choo Y, Klug A (2001) Design of polyzinc finger peptides with structured linkers. Proc Natl Acad Sci USA 98: 1432-1436

Natkunarajah M, Trittibach P, McIntosh J, Duran Y, Barker SE, Smith AJ, Nathwani AC, Ali RR (2008) Assessment of ocular transduction using single-stranded and self-complementary recombinant adeno-associated virus serotype 2/8. Gene Ther 15: 463-467

Nguyen M, Huan-Tu G, Gonzalez-Edick M, Rivera VM, Clackson T, Jooss KU, Harding TC (2007) Rapamycin-regulated control of antiangiogenic tumor therapy following rAAV-mediated gene transfer. Mol Ther 15: 912-920

O'Reilly M, Palfi A, Chadderton N, Millington-Ward S, Ader M, Cronin T, Tuohy T, Auricchio A, Hildinger M, Tivnan A, et al (2007) RNA interference-mediated suppression and replacement of human rhodopsin in vivo. Am J Hum Genet 81: 127-135

Pearson H (2008) Protein engineering: the fate of fingers. Nature 455: 160-164

Rebar EJ, Huang Y, Hickey R, Nath AK, Meoli D, Nath S, Chen B, Xu L, Liang Y, Jamieson AC, et al (2002) Induction of angiogenesis in a mouse model using engineered transcription factors. Nat Med 8: 1427-1432

Rehemtulla A, Warwar R, Kumar R, Ji X, Zack DJ, Swaroop A (1996) The basic motif-leucine zipper transcription factor Nrl can positively regulate rhodopsin gene expression. Proc Natl Acad Sci USA 93: 191-195

Sanges D, Comitato A, Tammaro R, Marigo V (2006) Apoptosis in retinal degeneration involves cross-talk between apoptosis-inducing factor (AIF) and caspase-12 and is blocked by calpain inhibitors. Proc Natl Acad Sci USA 103: 17366-17371

Segal DJ, Barbas CF, III (2001) Custom DNA-binding proteins come of age: polydactyl zinc-finger proteins. Curr Opin Biotechnol 12: 632-637

Segal DJ, Dreier B, Beerli RR, Barbas CF, III (1999) Toward controlling gene expression at will: selection and design of zinc finger domains recognizing each of the 5′-GNN-3′ DNA target sequences. Proc Natl Acad Sci USA 96: 2758-2763

Seipel K, Georgiev O, Schaffner W (1992) Different activation domains stimulate transcription from remote ('enhancer') and proximal ('promoter') positions. EMBO J 11: 4961-4968

Sohocki MM, Daiger SP, Bowne SJ, Rodriquez JA, Northrup H, Heckenlively JR, Birch DG, Mintz-Hittner H, Ruiz RS, Lewis RA, et al (2001) Prevalence of mutations causing retinitis pigmentosa and other inherited retinopathies. Hum Mutat 17: 42-51

Stieger K, Colle MA, Dubreil L, Mendes-Madeira A, Weber M, Le Meur G, Deschamps JY, Provost N, Nivard D, Cherel Y, et al (2008) Subretinal delivery of recombinant AAV serotype 8 vector in dogs results in gene transfer to neurons in the brain. Mol Ther 16: 916-923

Wright AF, Chakarova CF, Abd El-Aziz MM, Bhattacharya SS (2010) Photoreceptor degeneration: genetic and mechanistic dissection of a complex trait. Nat Rev 11: 273-284

Xia H, Mao Q, Eliason SL, Harper SQ, Martins IH, Orr HT, Paulson HL, Yang L, Kotin RM, Davidson BL (2004) RNAi suppresses polyglutamine-induced neurodegeneration in a model of spinocerebellar ataxia. Nat Med 10: 816-820

Zhang L, Spratt SK, Liu Q, Johnstone B, Qi H, Raschke EE, Jamieson AC, Rebar EJ, Wolffe AP, Case CC (2000) Synthetic zinc finger transcription factor action at an endogenous chromosomal site. Activation of the human erythropoietin gene. J Biol Chem 275: 33850-33860